

# A MULTIRATE RECURSIVE ARX ALGORITHM FOR ENERGY EFFICIENT WIRELESS STRUCTURAL MONITORING

R.A. Swartz and J.P. Lynch  
*University of Michigan, Ann Arbor, MI 48109-2125 USA*  
*asgard@umich.edu, jerlynch@umich.edu*

## Abstract

Wireless sensor networks enjoy significant cost savings and performance benefits over traditional cable-based sensor networks. Wireless structural monitoring systems for civil structures are both more cost-effective to install and offer features such as local data processing capabilities. One drawback associated with wireless sensors is their dependence on battery power. As such, the operational strategies that dictate the use of battery-powered wireless sensors are often focused on offering energy efficient unattended operation in the field. In this paper, an energy efficient system identification scheme is presented for wireless sensors designed for structural monitoring applications. The wireless sensor, termed Narada, is programmed to initiate the calculation of recursive ARX models at high sampling rates, then change to lower sampling rates by transforming system poles and zeros to the continuous-time domain and back to the discrete-time domain by use of the bilinear transform. This approach saves scarce battery energy by reducing the power demands of the analog-to-digital conversion process and reducing the number of calculations needed to calculate an accurate ARX model of the structural system.

## Introduction

For any developed nation, its civil infrastructure is a critical asset that can impact daily life and economic activities if compromised. Monitoring of these vital structures is often conducted in a haphazard manner; facility managers and owners largely rely on schedule-based visual inspection methods to monitor their assets. In some cases, a schedule-based inspection regimen may be excessively frequent and uneconomical, while in other cases, it may be too infrequent. In contrast, condition-based monitoring becomes possible with a permanently installed monitoring system that can trigger an alert when significant changes in the structural properties of the system are detected. Despite their tremendous societal importance, large amounts of funding are rarely available for monitoring civil structures. Installing a monitoring system on a large structure using traditional cable-based sensor networks is prohibitively expensive. For example, Celebi (2002) found that the installation of a cable-based system costs on the order of a few thousand dollars per channel. Using wireless sensors, large dense arrays of sensors can be installed at a fraction of the cost of a sparser cabled system. Wireless sensors are limited however, by bandwidth and battery power. Due to bandwidth limitations, it is often impossible to transmit every data point of every sensor channel to a central computer for processing when the network is large. Also, because wireless data transmission is an energy intensive process, battery life considerations limit the amount of data that can be transmitted before batteries must be replaced. As demonstrated by Straser and Kiremidjian (1998) and Lynch, et al (2004) wireless sensing units with on-board data processing abilities can be used to alleviate these problems. By locally performing modal analysis or executing structural health monitoring algorithms directly at the wireless sensor unit, the demand for bandwidth and energy can be significantly reduced, Lynch, et al (2004).

This paper proposes an energy-efficient wireless structural monitoring algorithm to be embedded within a wireless sensing unit. A wireless sensing prototype developed at the University of Michigan, named "Narada," is considered in this study (Figure 1). This algorithm employs a recursive auto-regressive with exogenous inputs (ARX) model that, for accuracy, is formulated using a sampling rate that is relatively high compared to the dynamics of the given system. After determining ARX coefficients and establishing that they do not change significantly over time, the unit may change to a slower sampling rate, thereby reducing demand on the wireless sensor's analog-to-digital converter (ADC) resulting in a corresponding reduction in the power consumed by both the microprocessor and the ADC. Lowering the

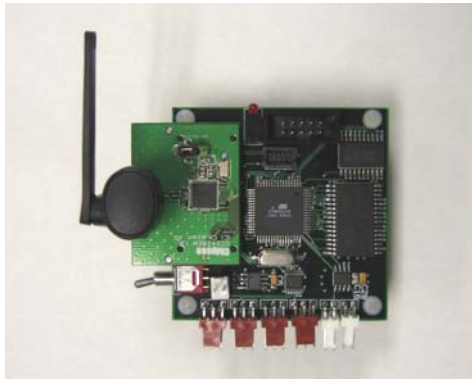


Figure 1. Narada wireless sensing unit

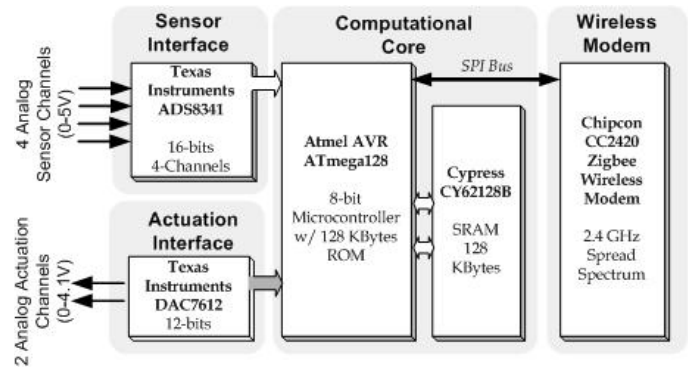


Figure 2. Narada functional diagram

sampling rate will result in a minor loss of precision within the system identification model, but for structural health monitoring applications that loss may be acceptable if the model is still precise enough to detect changes in the system that correspond to damage. Conversion of the ARX coefficients from high to low sampling rates is achieved through use of the bilinear transform. Having the ARX coefficients at the high sampling rate, a linear difference equation estimator that relates the dynamic system's inputs and outputs can be formed. Transforming the linear difference equation into the  $z$ -domain yields the poles and zeros of the estimator. The bilinear transform is then employed to convert the discrete poles and zeros to continuous time poles and zeros in the Laplace domain, using the current (high) sampling period. Using the desired new (low) sampling period, this algorithm again employs the bilinear transform to convert the estimator poles and zeros back to the  $z$ -domain. After the conversion, the recursive ARX algorithm continues. The performance of the estimator is evaluated by a data fit criterion based on the estimator error. Should the low rate estimator prove to be unsatisfactory, the wireless sensor could convert the ARX parameters back to the original high sampling rate to refine the model.

The multi-rate ARX algorithm will be embedded in the computational core of the Narada wireless sensing unit under development at the University of Michigan. The Narada unit has at its core an Atmel Atmega128 microprocessor with an additional 128kB of SRAM for computation and data storage. Its communication interface consists of the Chipcon CC2420 IEEE 802.15.4 compliant wireless radio. It has a four channel, 16-bit Texas Instruments ADS8341 ADC for data acquisition, and a two channel, 12-bit Texas Instruments DAC7612 digital-to-analog converter (DAC) for actuation. A functional diagram of the Narada unit can be found in Figure 2.

The remainder of this paper is structured as follows: the recursive ARX algorithm is presented. The use of the bilinear transform for frequency conversion follows with a demonstration of the performance of the converted estimator. Next, a brief overview of the battery energy preserved by using the reduced sample rate model on the Narada sensing unit will be presented. Finally, the potential for this algorithm for use in structural monitoring applications and for energy-aware battery powered wireless sensors is discussed.

## Recursive ARX

The recursive single-input single-output (SISO) ARX algorithm presented herein comes from the classical least-squares filter as presented by Juang (1994). In this formulation, the linear difference equation is expressed as:

$$y(k) + \sum_{i=1}^p Y_i^{(2)} y(k-i) = \sum_{i=1}^p Y_i^{(1)} u(k-1) + Du(k) \quad (1)$$

where  $p$  is the order of the model,  $k$  is the current time step,  $u$  and  $y$  are the system input and output respectively,  $Y_i^{(1)}$  and  $Y_i^{(2)}$  are the observer parameters, and  $D$  is the direct transmission term multiplying the current input. In compact matrix form, the relationship is

$$y(k) = \mathbf{Y}_p \mathbf{v}_p(k-1) \quad (2)$$

where

$$\mathbf{v}_p(k-1) = \begin{bmatrix} u(k) \\ y(k-1) \\ u(k-1) \\ \vdots \\ y(k-p) \\ u(k-p) \end{bmatrix}, \quad \mathbf{Y}_p = \begin{bmatrix} D & -Y_1^{(2)} & Y_1^{(1)} & \dots & -Y_p^{(2)} & Y_p^{(1)} \end{bmatrix}. \quad (3)$$

Finding  $\mathbf{Y}_p$  recursively avoids the requirement for inverting a large input/output matrix which saves computational steps and preserves accuracy as matrix conditioning can lead to errors in the matrix inversion. Information is carried in a  $2p+1$  by  $2p+1$  (assuming a SISO system)  $\mathbf{P}_p$  matrix that must be updated recursively (see Juang (1994) for the formulation). To initialize the system, a good estimate for  $\mathbf{Y}_p$  and  $\mathbf{P}_p$  derived from experience with the system in question can be used. Lacking that, Juang (1994) suggests initializing with all  $\mathbf{Y}_p$  elements equal to zero and  $\mathbf{P}_p$  equal to  $d^* \mathbf{I}$  where  $d$  is some arbitrary large number and  $\mathbf{I}$  is the identity matrix. Once initialized, the recursive ARX steps are as follows. Update  $\mathbf{v}_p$  with data from the current time step. Define:

$$\mathbf{G}_p(k) = \frac{\mathbf{v}_p^T(k) \mathbf{P}_p(k-1)}{1 + \mathbf{v}_p^T(k) \mathbf{P}_p(k-1) \mathbf{v}_p(k)} \quad (4)$$

$$\hat{y}(k+1) = \hat{\mathbf{Y}}_p(k) \mathbf{v}_p(k) \quad (5)$$

where  $\hat{y}(k+1)$  is the estimated output at step  $k+1$  and  $\hat{\mathbf{Y}}_p$  is used instead of  $\mathbf{Y}_p$  to indicate the estimated ARX model coefficients. Then update

$$\mathbf{P}_p(k) = \mathbf{P}_p(k-1) [\mathbf{I} - \mathbf{v}_p(k) \mathbf{G}_p(k)] \quad (6)$$

and

$$\hat{\mathbf{Y}}_p(k+1) = \hat{\mathbf{Y}}_p(k) + [y(k+1) - \hat{y}(k+1)] \mathbf{G}_p(k). \quad (7)$$

When new data becomes available, advance  $k$  to the next time step and return to the beginning of the loop. To measure the performance of the estimator at each step, the following metric is adapted from Ljung (1999).

$$J_p(k) = \frac{1}{k} \sum_{i=1}^k |y(i) - \hat{y}(i)|^2 \quad (8)$$

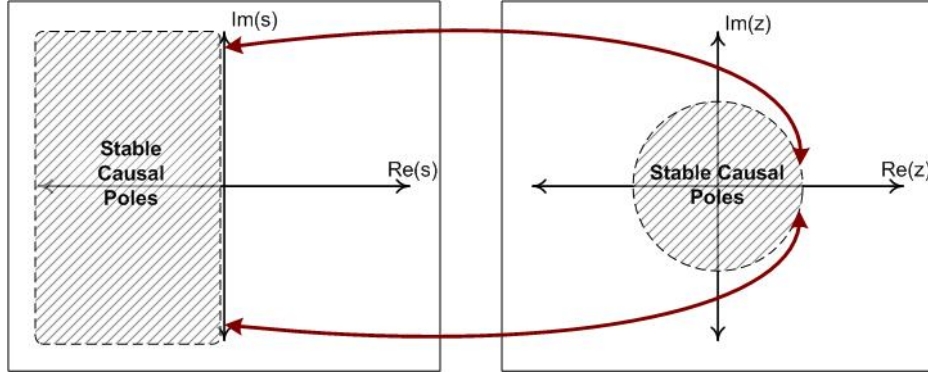


Figure 3. The Bilinear Transform

### Sampling Rate Conversion

Operating at a high sampling rate for the lifetime of the wireless sensor is a constant drain on battery power. One important means of extending battery life is the use of a sleep mode for the wireless sensor where most functions are shut down when the unit is not required to be running. If the unit can run at a slower sampling rate when fully powered up, additional improvements in battery life can be attained. The problem is how to correlate information obtained at the high rate to that at the low rate to best take advantage of all of the available data. For this study, recursively obtained ARX coefficients for a two degree model,  $p=2$ , are converted from one arbitrary sampling rate to another by use of the bilinear transform. The bilinear transform is a mapping of the left-hand side of the continuous-time complex plane ( $s$ , Laplace transform complex variable) into the unit circle of the discrete-time complex plane ( $z$ , Z-transform complex variable) as shown in Figure 3.

For stable observer poles with frequencies that are small compared to the sampling rate, this mapping results in minimal distortion. The bilinear transform has the additional advantage of being a one-to-one mapping eliminating the possibility for aliasing, (Oppenheim 1999). A Z-transform of the linear difference equation given in (1) for the two degree model yields

$$\frac{y(z)}{u(z)} = \frac{D + \hat{Y}_1^{(1)} z^{-1} + \hat{Y}_2^{(1)} z^{-2}}{1 + \hat{Y}_1^{(2)} z^{-1} + \hat{Y}_2^{(2)} z^{-2}} \quad (9)$$

To map the poles and zeros represented by this equation into the continuous-time Laplace domain, the bilinear relationship between the  $s$  and  $z$  complex variables can be employed:

$$z = \frac{2 + sT_s}{2 - sT_s} \quad (10)$$

where  $T_s$  is the current sampling period. After some algebraic manipulation, it is possible to obtain

$$\frac{y(s)}{u(s)} = \frac{-T_s^2 (D - \hat{Y}_1^{(1)} + \hat{Y}_2^{(1)})s^2 - 4T_s (D - \hat{Y}_2^{(1)})s - 4(D + \hat{Y}_1^{(1)} + \hat{Y}_2^{(1)})}{-T_s^2 (1 - \hat{Y}_1^{(2)} + \hat{Y}_2^{(2)})s^2 - 4T_s (1 - \hat{Y}_2^{(2)})s - 4(1 + \hat{Y}_1^{(2)} + \hat{Y}_2^{(2)})} \quad (11)$$

To map back to the discrete-time  $z$ -domain, use the new desired sampling period  $T_s'$  and substitute

$$s = \frac{2}{T_s'} \frac{1 - z^{-1}}{1 + z^{-1}} \quad (12)$$

into (10). After some algebraic simplifications, the result produces an equation in the form of:

$$\frac{y(z)}{u(z)} = \frac{D' + \hat{Y}_1^{(1)'} z^{-1} + \hat{Y}_2^{(1)'} z^{-2}}{1 + \hat{Y}_1^{(2)'} z^{-1} + \hat{Y}_2^{(2)'} z^{-2}} \quad (13)$$

where the new vector of ARX parameters is

$$\hat{\mathbf{Y}}_p' = \begin{bmatrix} D' & -\hat{Y}_1^{(2)'} & \hat{Y}_1^{(1)'} & \dots & -\hat{Y}_p^{(2)'} & \hat{Y}_p^{(1)'} \end{bmatrix} \quad (14)$$

The resulting expressions for the elements of  $\hat{\mathbf{Y}}_p'$  in terms of the original ARX coefficients and the sampling periods,  $T_s$  and  $T_s'$ , can thus be obtained but are excessively lengthy to display in this space.

## Method Validation

To validate this conversion method, data obtained by prototype wireless sensing units installed on a three story shake table test structure located at the National Center for Research in Earthquake Engineering (NCREE) at National Taiwan University (see Figure 4) is used. The model uses acceleration data from the base as the input, and acceleration data for floors 1, 2, or 3 as the output; for simplicity, only one output is considered at a time. To demonstrate the effectiveness of this method, a second order ( $p=2$ ) ARX model of the system for a given floor output is created using the recursive algorithm initialized generically, with the initial ARX parameters equal to zero and the  $\mathbf{P}_p$  matrix equal to  $100 \cdot \mathbf{I}$ . Partway through, the data is downsampled (from 200 to 100 Hz) and the ARX coefficients are converted to the downsampled rate with the bilinear transform. The recursive ARX algorithm is initialized with the converted ARX parameters and continued. A plot of the measured data and the estimated data versus time is shown in Figure 5 along with the five ARX parameters for comparison. Note the shift in the ARX parameters at the time step (at ~11 sec) that the shift in sampling rate is made indicating the bilinear transform conversion. The error metric in (8) is plotted versus time in Figure 6 for a number of cases. The lowest final value for the error metric, as expected, is obtained using the highest sampling rate for the entire length of the data set. Also plotted is the performance for the recursive estimator on the downsampled data set with generic initialization which has a higher final error value. Between those two curves is the error curve from the recursive ARX estimator on the downsampled data set using the bilinearly transformed ARX numbers as initial values. Also plotted for comparison, is the error result for the same data set using a static estimator derived from the bilinearly transformed ARX numbers.

Changing sampling rates partway through this data set should yield error metrics that vary between the generically initialized downsampled set and the generically initialized full data set. Figure 7 presents the resulting final error metric value for the estimator for a large number of runs as it is forced to change sampling rates at progressively later points through the data set. The same data set is used for all runs for consistency. As the algorithm is allowed to run at the high sampling rate longer, the error drops off rapidly at first, then asymptotically approaching the full-length, high sampling rate value. Warping errors in the ARX parameter conversion do cause a noticeable increase in error for very early sampling rate conversions.



**Figure 4. Three story test structure**

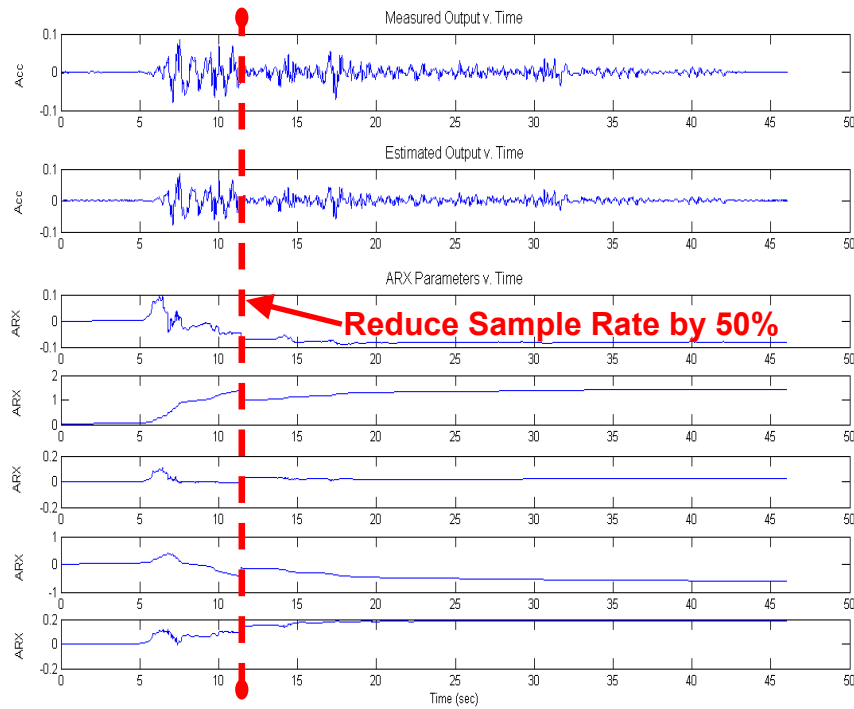


**Figure 5. Estimator performance**

## Energy Considerations

Performing the recursive ARX operation in real time is an energy drain for a wireless sensor. The motivation for reducing the sampling rate is to reduce the number of operations required of the wireless sensor while trading some accuracy. This paper considers the potential energy savings for the University of Michigan Narada unit. It is the power consumption of the ADC during sampling and of the microprocessor for calculating the recursive algorithm that is of interest.

When the ADS8341 is in auto power-down mode, the amount of current required for operation is a log function of the sampling rate when the clock source is held constant. The smaller the ratio of sampling frequency to clock frequency, the lower the power draw. On the Narada, the ADC is connected to the SPI bus of the microprocessor which maintains a 1.0GHz clock signal. Sampling two channels, one input and one output, at a rate of 500Hz, for example, requires about  $10\mu\text{A}$  of current. Cutting the rate in half reduces the current requirement to  $6\mu\text{A}$ . At a supply voltage of 5V, this is an energy savings of 2mW.

On the microprocessor side, reducing the sampling rate reduces the number of computations required to update the recursive ARX parameters. A summary of the minimum processor requirements per data sample collected is presented in Table 1; this corresponds to the energy consumption by the microprocessor. The values in this table show the number of operations required to update the various quantities, as well as the expected number of clock cycles the processor would require to perform these operations. Table 1 also summarizes the number of operations and clock cycles

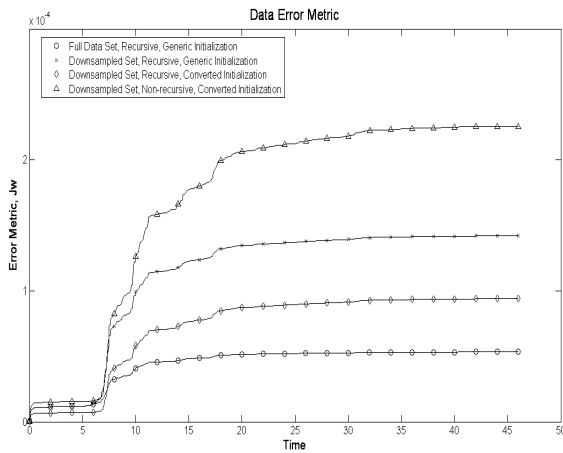


**Figure 6. Error metric comparison**

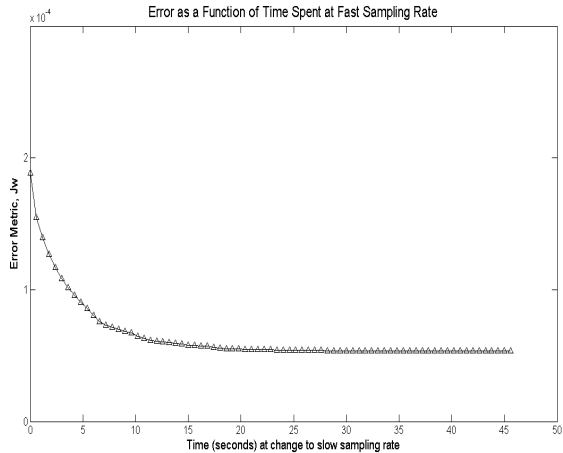


**Figure 7. Error metric trendline**

required to make the decision to change rates and to convert the ARX parameters from one sampling rate to another. Note that those numbers are for the case of predetermined, hard-coded sampling rates.

Assuming 900 computational clock cycles per time step, and a scaled clock source of 2.0Gz, the processor is required to devote 22.5% of its potential cycles to recursive ARX computations at 500Hz. Reducing the sampling rate in half will cut the number of clock cycles required for computations in half thereby reducing the energy requirements for the microprocessor.

## Conclusions

Reducing the sampling rate for any monitoring activity reduces the energy demand and can extend the battery life of a wireless sensor; this reduction in energy comes at the expense of accuracy, however. This study demonstrates how, for ARX modeling, it is possible to take advantage of the information acquired at the high sampling rate to improve the accuracy of the model at the lower sampling rate. By using a recursive algorithm, large matrix inversions can be avoided. An additional advantage of the recursive algorithm is that distortions in the pole/zero locations introduced by warping in the bilinear transform will be filtered out over time. This algorithm shows promise for structural monitoring applications. Changes in the ARX parameters over time or large errors in the estimated output values can be an indication of changes within the system that might indicate damage (Farrar and Sohn 2001). The capability to change sampling rate down is useful to save energy, but the ability to change sampling rate up is also useful to better capture high frequency effects. Future work in this area should include exploring recursively updated, multi-rate models for system ID as well as damage detection and cooperative sampling rate determination between multiple nodes.

| Operation   | Shifting | Compare<br>if | Float Ops |          |            | Clock Cycles |
|---|----------|---------------|-----------|----------|------------|--------------|
|   |          |               | Add       | Multiply | Divide     |              |
| <b>Recursive ARX</b>                              |          |               |           |          |            |              |
| update $v_p$                                      | 6        |               |           |          |            | 6            |
| update error                                      |          |               | 1         |          |            | 2            |
| update $\hat{Y}_p$                                | 25       |               | 5         | 5        |            | 65           |
| update $\mathbf{temp}_1$ , part of $\mathbf{G}_p$ |          |               | 20        | 25       |            | 190          |
| update $\mathbf{temp}_2$ , part of $\mathbf{G}_p$ |          |               | 5         | 5        |            | 40           |
| update $\mathbf{G}_p$                             |          |               |           |          | 5          | 65           |
| update $\hat{y}$                                  |          |               | 4         | 5        |            | 38           |
| update $\mathbf{temp}_3$ , part of $\mathbf{P}_p$ |          |               | 25        | 25       |            | 200          |
| update $\mathbf{P}_p$                             | 50       |               | 25        | 25       |            | 250          |
|   |          |               |           |          | <b>SUM</b> | 856          |
| <b>Check Rate Change Criterion</b>                |          |               |           |          |            |              |
| check high/low                                    |          | 1             |           |          |            | 4            |
| calc error metric, $J_w$                          | 2        |               | 2         | 1        | 1          | 25           |
| check threshold                                   |          | 1             |           |          |            | 4            |
|   |          |               |           |          | <b>SUM</b> | 33           |
| <b>Convert ARX Parameters</b>                     |          |               |           |          |            |              |
| calc initial parameters                           |          |               | 18        | 18       |            | 144          |
| find $\hat{Y}'_p$                                 |          |               |           |          | 5          | 65           |
|   |          |               |           |          | <b>SUM</b> | 209          |

**Table 1. Computational demand summary**

### Acknowledgements

Direct support for this study has been provided by the National Science Foundation (Grants CMS-0421190 and CMS-0528867). Additional support was provided by the National Center for Research on Earthquake Engineering (NCREE) and the Rackham Grant and Fellowship Program at the University of Michigan. The authors would like to express their gratitude to Prof. Kincho H. Law and Mr. Yang Wang, Stanford University, and Prof. Loh, National Taiwan University, who have been instrumental in all facets of this research project.

### References

- Celebi, M. (2002), "Seismic Instrumentation of Buildings (with Emphasis of Federal Buildings)," *Report No. 0-7460-68170* United States Geological Survey (USGS), Menlo Park, California.
- Straser, E. G., A. S. Kiremidjian (1998), "A Modular, Wireless Damage Monitoring System for Structures," *Report No. 128*, John A. Blume Earthquake Engineering Center, Department of Civil and Environmental Engineering, Stanford University, Stanford, California.
- Lynch, J.P., A. Sundararajan, K.H. Law, A.S. Kiremidjian, E. Carryer (2004), "Embedding Damage Detection Algorithms in a Wireless Sensing Unit for Attainment of Operational Power Efficiency," *Smart Materials and Structures, IOP*, **13**(4): 800-810.
- Juang, J. (1994), *Applied System Identification*, Prentice Hall PTR, Upper Saddle River, New Jersey.
- Ljung, L. (1999), *System Identification Theory for the User*, Prentice Hall PTR, Upper Saddle River, New Jersey.
- Oppenheim, A., R. Schaffer, J. Buck (1999), *Discrete-Time Signal Processing*, Prentice Hall PTR, Upper Saddle River, New Jersey.
- Sohn, H., C. Farrar (2001), "Damage diagnosis using time series analysis of vibration signals," *Smart Materials and Structures*, **10**(3), 446-451.